5-2021

Studies of the dUTPase of the Western Corn Rootworm

Carlos Riera-Ruiz
University of Nebraska-Lincoln, criera-ruiz@huskers.unl.edu

Studies of the dUTPase of the Western Corn Rootworm

By

Carlos A. Riera-Ruiz

A THESIS

Presented to the Faculty of

The Graduate College at the University of Nebraska

In partial Fulfillment of Requirements

For the Degree of Master of Science

Major: Biological Sciences

Under the Supervision of Professor Hideaki Moriyama

Lincoln, Nebraska

May 2021

Studies of dUTPase enzyme of the Western Corn Rootworm

Carlos Riera-Ruiz, M.S.

University of Nebraska, 2021

Advisor: Hideaki Moriyama

The western corn rootworm (WCR), *Diabrotica virgifera virgifera*, is a major corn pest in the United States and Europe. WCR has developed resistance to multiple management strategies, including Cry proteins. Even though the biology and ecology have been thoroughly studied in WCR, their genome and molecular mechanisms are understudied. This work focuses on the ubiquitous enzyme deoxyuridine triphosphatase (dUTPase) encoded by the DUT gene. dUTPase hydrolyzes dUTP into dUMP and pyrophosphate. It contributes to genome stability by keeping the uracil-to-thymine ratio at a certain level. In WCR, two dUTPase isoforms were predicted using transcriptome analyses. These two potential isoforms shared the core part of the enzyme including five conserved motifs forming active sites while they differed in the amino-termini. To assess the enzymatic activity and substrate specificity, the core sequence of the WCR dUTPase gene was cloned, expressed in *Escherichia coli*, and purified. The WCR dUTPase hydrolyzed dUTP but not dATP, dTTP, dCTP or dGTP. Structural analysis showed that Lys92 on WCR dUTPase seemed to govern the substrate specificity. This study revealed the properties of key pyrimidine metabolism partly of WCR and provided the basis for future studies.

AKCNOWLEDGEMENTS

I would like to acknowledge the people who contributed toward completion of this degree and my professional growth. Thanks to my advisor, Dr. Hideaki Moriyama, for giving me the opportunity to learn from him, his advice and for encouraging me to be open to new challenges. Thanks to Dr. Etsuko Moriyama for opening me the doors of her lab and guiding me during my first year. Thanks to her lab members, especially Dr. Sairam Behera for his valuable advice. Thanks to Dr. Ana Velez and her lab members for their support during hard times and openness to collaborate in our projects. I would also like to acknowledge the support and words of wisdom from Dr. Tomáš Helikar and Dr. Joe Louis. Lastly, I would like to acknowledge the significant role of my family and friends, whose support kept me sane during this adventure (most of the time).

I would also like to acknowledge the institutions that gave me the opportunity to pursue my graduate studies: Escuela Superior Politécnica del Litoral, through the "Waler Valdano Raffo" program and Centro de Investigaciones Biotecnológicas del Ecuador; the Fulbright commission in Ecuador; and the School of Biological Sciences at the University of Nebraska-Lincoln.

Table of contents

Figures

Tables

1. Literature Review

1.1. The Western Corn Rootworm

Diabrotica virgifera virgifera LeConte (Coleoptera: Chrysomelidae), the Western Corn Rootworm (WCR). *Diabrotica* species are responsible for greater than $2 billion in annual losses in control costs and yield losses [1]. Currently, multiple management strategies are used to mitigate WCR including cultural control, synthetic insecticides, and transgenic corn [2]. However, WCR has developed resistance to many of the current management strategies [2], [3]. One of the most successful control strategies involves the transgenic expression of Cry toxins from the bacterium *Bacillus thuringiensis*, in commercial corn lines commonly known as Bt corn [4]. Cry toxins are produced and are known to cause pores in the membranes of the insect midguts. However, resistant populations of WCR to Cry proteins Cry3Bb1 and mCry3A have already been reported [5], [6], including WCR populations from Nebraska [7]. Given the evolution of resistance to multiple management strategies in WCR it is fundamental to develop new management strategies to control WCR but new cry proteins are being engineered using DNA shuffling to increase solubility and toxicity against WCR [8] and RNA interference (RNAi) technology will be soon released for the management of this insect pest [9].

1.2. The Pyrimidine metabolism

1.2.1. Pyrimidine homeostasis

The pyrimidine metabolism is conserved among species and likely contains lethal genes. In prokaryotes, aspartate transcarbamylase (ATCase) is the first enzyme of the pyrimidine metabolism [10], [11]. However, in eukaryotes, ATCase is replaced by a multifunctional enzyme with carbamoyl-phosphate synthetase, aspartate transcarbamylase, and dihydroorotase activity (CAD), with size of of 240 kDa. These are the first steps in the pyrimidine metabolism of eukaryotes [12]–[14]. The reactions catalyzed by dihydroorotate dehydrogenase (DODH), Uridine monophosphate synthase (UMPS) and uridine monophosphate kinase (UMPK) are necessary to obtain uridine monophosphate (UMP) (**Figure 1**). After the synthesis of UMP, cells can directly phosphorylate it and obtain di- and tri-phosphate uracil nucleotides. However, to obtain uracil deoxynucleotides, cytosine deoxynucleotide must be available. Cytidine triphosphate synthase (CTP synthase) adds an amino group to the uracil moiety of uracil triphosphate (UTP) to produce cytidine triphosphate (CTP) [15] from which deoxycytidine triphosphate (dCTP) or deoxycytidine monophosphate (dCMP) can be obtained. In higher organisms, dCMP is deamidated to obtain deoxy uracil monophosphate (dUMP) and subsequently deoxy thymidine monophosphate (dTMP) by a reaction catalyzed by thymidylate kinase (TYMK) [16] (**Figure 1**).

Pyrimidine homeostasis is a key factor in regulation. Nucleotides are the subunits of nucleic acids. They also perform functions as coenzymes and regulators, and have a role for anabolic purposes [17]. For example, enzymes containing

pyrimidine-binding sites have been proposed to be regulated by the pyrimidine biosynthesis, such as the ATCase. ATCase regulates the rate of purines and pyrimidines production. When the pyrimidines, such as CTP, binds to ATCase, it changes to the T state of ATCase suppressing the pyrimidine pathway [18]. Thus, ATCase links the pyrimidine and purine pathways and the synthesis of their final products.

1.2.2. dUTPase

Deoxyuridine triphosphatase (dUTPase) is a key enzyme in the pyrimidine metabolism. It is encoded by the DUT gene. dUTPase is an essential enzyme for free-living organisms. The sole knockdown of dUTPase causes death to *Saccharomyces cerevisiae* [19] and *E. coli* [20]. dUTPase has a dual role in the cells. First, it enables the production of thymidine by making dUMP available, the substrate for deoxythymine triphosphate (dTTP) synthesis. Second, it keeps uracil out of DNA. The latter role has evolved to solve a structural-born issue: uracil (U) and thymine (T) are structurally similar pyrimidines, and most DNA polymerases cannot distinguish between them. Thus, uracil can easily be misincorporated to DNA molecules by DNA polymerase (δ and ε in eukaryotes). One of the main roles of dUTPase is to keep a low ratio of U/T by constantly catalyzing the hydrolyzation of dUTP to dUMP. This minimizes the misincorporation of uracil into DNA by making dUTP virtually unavailable. This aspect of the pyrimidine metabolism has been exploited in cancer chemotherapy to prevent tumor growth [21]. Increased expression of dUTPase has been associated with poor efficiency of 5Fu-based chemotherapy. Thus,

pharmacological inhibition of dUTPase has been suggested as an alternative approach for chemotherapy [22]. Expression of dUTPase is fine tuned in *Drosophila melanogaster* to meet DNA synthesis requirements in specific tissues [23]. However, it is unknown how the modulation of dUTPase expression can affect the pyrimidines pool in WCR cells and how it affects the regulation of other enzymes.

1.2.3. dUTPase mechanism

dUTPase is a hydrolase and has the EC number 3.6.1.23. The main mechanism is a nucleophilic attack of a catalytic water molecule on the α-phosphate of dUTP (**Figure 2**). In the transition state water deprotonation by an Asp residue (shown as PT, proton transfer, in Figure 2) triggers the attack to the α-P. A pentacovalent intermediate is formed (α-P center) due to the nucleophilic attack (shown as ET, electron transfer). The last electron transfer breaks the α-β phosphate bridge. Finally, the pyrophosphate (not shown) and dUMP are released [24]. One of the inhibitors for this enzyme is 2′-deoxyuridine 5′-[(α,β)-imido]-triphosphate [25]. It is similar to the native substrate, dUTP (**Figure 3**). The difference between the inhibitor and dUTP is in the imido group in the α-β phosphate bridge, which prevents hydrolysis. 2′-deoxyuridine 5′-[(α,β)-imido]-triphosphate is a competitive inhibitor (Ki is 5μM [26]) because it is similar to the substrate of the enzyme.

2. MATERIALS AND METHODS

2.1. Sequence analysis

2.1.1. Identification of isoforms

The contigs potentially encoding the transcripts of dUTPase from *Diabrotica virgifera virgifera* LeConte (WCR; western corn rootworm) [27] were identified by TBLASTN searches (v2.8.1+) [28] using the dUTPase protein sequences of three coleopterans and a dipteran (**Table 1**). Those dUTPase transcripts were mapped on the genomic sequence of *D. v. virgifera* (GenBank Locus, ML015595.1) using MAFFT v7.419 with the default parameters [35]. The canonical GT–AG flanking regions were located for each intron–exon boundary. The genomes of other insects including *Anoplophora glabripennis* (XP_018573994.1), *Tribolium castaneum* (XP_973701.1), *Leptinotarsa decemlineata* (XP_023012863.1), and *Drosophila melanogaster* isoforms A (NP_609479.1) and B (NP_723647.1) were also used as references to find dUTPase genes and map the transcripts to find exon-intron boundaries.

2.1.2. Sequence alignment

The dUTPase protein sequences from the WCR contig 1, human (PDB ID, 3ehw), and *D. melanogaster* (UniProt ID, Q9V3I1) were aligned by the T-coffee server [29].

2.2. 3D-structural analysis

3D-structural models of the WCR dUPTase were built using the SWISS-MODEL server [30] utilizing the 3D-structure of the human dUTPase (Hs; PDB ID, 3ehw) as the template, which was top-ranked by the server. Models of the dUTPases

for WCR contig1 (WCR1) and the Arg70Lys mutant (WCR_C) resulted in the QMEAN values at –0.3 and –0.35, respectively. Contig2 (WCR2) was not used for 3D-structural analysis because both contig1 and contig2 share the C-terminus with the motifs forming the active site. The amino-terminus is likely involved in subcellar localization which is not the focus of this work. The root-mean-square deviations (RMSDs) between α-carbons in dUTPase pairs WCR1–Hs and WCR_C–Hs were both 0 Å. The RMSD between the WCR1 and WCR_C dUTPases was 0.000 Å. The 3D-model of *D. melanogaster* dUTPase (Dm; UniProt ID, Q9V3I1) received a QMEAN value of –0.40. The RMSDs for Hs and WCR1 against Dm were 0.064 Å and 0.20 Å, respectively. The QMEAN values indicate the “degree of nativeness” of the structural features [31], and SWISS-MODEL models are considered to be good when the QMEAN value remains within the range between 0 and 1. Models are usable when the RMSD between the model and template is less than 2 Å [32], [33]. Thus, the presented models are judged usable. Structural mining was performed using PyMOL (Version 2.0, Schrödinger, New York, NY, USA).

2.3. Protein Production and Purification

2.3.1. Gene construct

A DNA fragment encoding the WCR DUT gene was synthesized with the optimum codon utilization for *E. coli* by Gene Script (Piscataway, NJ, USA; Figure 4). The modified DUT gene sequence was cloned into pET-15 (Novagen, Madison, WI, USA) using the NcoI and XhoI sites. In addition to the codon usage, the resulting construct has two modifications. The first five amino acids,

MSPAN, of the dUTPase predicted isoform 1 were substituted with a sequence containing a 6-histidine tag and a thrombin cleavage site (MGSSHHHHHHSSGLVPRGS). An internal mutation, Arg70Lys in M2, was introduced to prevent secondary thrombin cleavage. The DNA sequences are presented in **Figure 4.**

2.3.2. Protein production

The WCR dUTPase was prepared as described [34]–[36]. Briefly, for a 200-ml TB media, 1% volume of bacteria was inoculated using an overnight culture of *E. coli* JM109 (DE3) harboring the construct and cultured at 37˚C. Protein production was induced by adding IPTG to reach 0.5 mM at an optical density of 0.5 at 600 nm. The culture was continued at 28˚C for 18 h. Bacteria were collected by centrifugation and disrupted by sonication.

2.3.3. Protein purification

The cleared lysate was subjected to a His-Trap HP Ni-NTA column chromatography (GE Healthcare, Piscataway, New Jersey, USA). The 6-histidine tag was cleaved from the recombinant protein by thrombin (Hematologic Technologies, Essex Junction, VT, USA). Digested proteins were passed through a His-Trap HP Ni-NTA column and a Benzamidine Sepharose column (GE Healthcare, Piscataway, New Jersey, USA). A 10 mg of WCR dUTPase was purified from 2.5 g of cells. Further purification was reached with Ion exchange chromatography using a Hi-Trap SP (GE Healthcare, Piscataway, New Jersey, USA). Finally, the sample was dialyzed against potassium phosphate buffer, pH 7.4.

2.3.4. Peptide identification by mass spectrometry

The purified WCR dUTPase was subjected to 18% SDS-PAGE. The band corresponding to ~15 kDa potentially corresponding to the dUTPase construct was cut and submitted for mass spectrometry at the University of Nebraska–Lincoln Proteomics and Metabolomic Research Core Facility (Lincoln, NE, USA). Briefly, the trypsin-digested sample was run by nanoLC-MS/MS using a 1h gradient on a 0.075 × 250 mm C18 column (Waters, Milford, MA, USA) feeding into a Q-Exactive HF mass spectrometer (Thermo Fisher). All MS/MS samples were analyzed using Mascot (Matrix Science, London, UK, v2.6.1) and set up to search the common contaminant database, cRAP_20150130.fasta (117 entries), and the SwissProt database, Release 2019_02 (559352 entries), assuming the digestion enzyme trypsin. Peptides were identified using the Peptide Prophet algorithm [37], [38].

2.4. Size analysis chromatography

The purified sample was concentrated using an Amicon Ultra-4 Centrifugal Filter Unit (MilliporeSigma, Burlington, MA, USA). The concentrated sample was subjected to a Superdex Matrix GE Healthcare (Piscataway, NJ, USA), and the molecular weight was calibrated using SEC standard (BioRad, Hercules, CA, USA).

2.5. Enzyme kinetics

Kinetic assay of the WCR dUTPase was performed according to [39]. Conventional assay was performed manually using Beckman Coulter DU-530 UV/Vis spectrophotometer (Palo Alto, California, USA). For a plastic cuvette

containing 5 µl of 1.1 µM WCR dUTPase, 2000 µl of 20 mM dUTP in 100 mM KCl, 5 mM $MgCl_2$, 0.025 mM cresol red, and 0.25 mM bicine pH 8.2. A decrease in absorbance was monitored at 572 nm for 60 s with recordings every 5 s. To assess the magnesium dependency of dUTPase, prior to the assay, enzyme was incubated with 0.5 or 5 mM EDTA for 10 min in iced water. To test the substrate specificity, dUTP was replaced with dATP, dTTP, dCTP, and dGTP. The automated stopped-flow equipment (Hi-Tech SF-61DX2, TgK Scientific, Bradford-on-Avon, UK) was used in the kinetic assay in higher dilution, where the concentrations for enzyme was 5×10^{-2} µM and for substrate were 1, 5, and 20 mM.

Absorbance data from each experiment was fitted to the function,

$$y = ae^{-xb} + c \qquad \text{(Eq. 1)}$$

where x and y denote time and absorbance, respectively. The predicted points were used to calculate the concentration of product formation at time t, $[P]_t$ using the below equation:

$$[P]_t = \frac{A_0 - A_t}{A_0 - A_\infty}[S]_0 \qquad \text{(Eq. 2)}$$

where $[S]_0$ is the substrate concentration, and A_0, A_t, and A_∞ correspond to the absorbance at the start, time *t,* and end of the reaction, respectively. The time

course reaction was calculated using the integrated Michaelis–Menten equation [40],

$$\frac{[P]_t}{t} = V - \frac{K}{t}\ln\frac{[S]_0}{[S]_0 - [P]_t} \qquad \text{(Eq. 3)}$$

where K and V denote K_m and V_{max}, respectively. Equations 2 and 3 were used to plot the graph of $\frac{[P]_t}{t}$ against $\frac{\ln\frac{[S]_0}{[S]_0-[S]_t}}{t}$. A linear regression was used to calculate the slope and intercept of the curve which gives the K_m and V_{max}, respectively, for each experiment. K_{cat} and K_{cat}/K_m were calculated using the propagation of error approach. The reported kinetic parameters resulted on the average of the three experimental conditions measured with the stopped-flow system. All calculations were done using R v3.5.3 (R Foundation, Vienna, Austria; /www.r-project.org).

2.6. Pathway analysis

In order to study the pyrimidine metabolism of the Western Corn Rootworm, we first annotated the proteins encoded in the genome (GCF_003013835.1) with the K orthology numbers using the GhostKoala server from KEGG [41]. The GhostKOALA was setup to search the KEGG genes in the ‘genus_prokaryotes + family_eukaryotes’ database. The KEGG Orthology tool was used to obtain the protein orthologs of two insects, *D. melanogaster* (dme) [42] and the red flour beetle *T. castaneum* (tca) [43], *E. coli* (eco) [44], and human (hsa). The set of orthologs were mapped against the reference pyrimidine metabolism (00240) using the KEGG Mapper - Reconstruct Pathway tool [45]. The orthologs

identified were verified by the reciprocal BLAST similarity search and completed by literature review.

3. RESULTS

3.1. WCR dUTPase is predicted to form two isoforms in WCR

From the WCR transcriptome, two contig sequences corresponding to the DUT gene sequence were found (**Figure 5**). The contig 1 had three exons and encoded 149 amino acids. The contig 2 was composed of four exons and encoded 169 amino acids. These contigs share the last two exons but differ at the amino-termini. The deduced amino acid sequences of isoforms contain the five canonical motifs M1–5 of trimeric dUTPases (**Figure 6**) [46]. In this study we focus on the contig 1.

3.2. WCR dUTPase structural insights

The sequence encoding dUTPase corresponding to the contig 1 was synthesized using the codon preference of *E. coli* and cloned into a pET15b vector (**Figure 4**). In this construction, dUTPase was produced as a 6-histidine-tagged protein (deduced mass: 17.5 kDa). After purification using a metal-affinity column, the 6-histidine tag was cleaved off by thrombin. The result of SDS-PAGE revealed that the purified protein had a molecular weight of ~15.6 kDa (**Figure 8A**). The identity of the purified protein as the WCR dUTPase was confirmed by tryptic mass spectrometry (**Figure 9**). Forty peptides were isolated after digestion with trypsin. Thirty-two of the fragments were exclusive to the amino acid sequence of the construct. Size analysis chromatography revealed that the mass of the WCR dUTPase was 48 kDa (**Figure 8B**). The estimated molecular weight was slightly higher than the triplicated monomer size. Taken together, these observations suggested that the WCR dUTPase takes a trimer format.

3.3. WCR dUTPase is specific for dUTP

Conventional cresol red assay showed purified dUTPase has activity (**Figure 10**, **Table 2**). When EDTA was added to achieve final concentration 0.5 mM, the color change of cresol red by hydrolyzation of dUTP was not observed (Figure 11, **Figure 12**). However, when the enzyme was subsequently incubated with $MgCl_2$ at a concentration of 5 μM, the enzyme activity was recovered. When the substrate was changed to either dCTP, dTTP, dATP, or dGTP, the color change was not detected in the conventional method or stopped flow after 60 (**Figure 13**). The enzyme kinetics assay of the WCR dUTPase was performed under multiple turnover conditions by the stopped-flow method [25]. The reaction trace was recorded with enzyme and substrate (dUTP) concentrations of 50 nM and 20 mM respectively (**Figure 10**), and V_{max} and K_M were estimated as 1.43 ± 0.03 μM/s and 0.7 ± 0.03 μM, respectively (**Table 2**).

4. DISCUSSION

4.1. Comparison of isoforms in relevant organisms.

Analyses of the WCR transcriptome revealed two transcripts of the DUT gene. We confirmed the enzymatic activity of the contig 1, which has three exons (**Figure 10**). Because the C-terminus contains the conserved motifs that form the active site we used for this study contig 1 only. The contig 2 shares the core domain with contig 1 (**Figure 5** and **Figure 6**) but includes an extra exon at the amino terminus which extra sequences likely contain a peptide motif involved in cellular localization. In *Drosophila* species, DUT isoforms are relevant to cellular localization of dUTPase. In *D. melanogaster*, nuclear and cytoplasmic dUTPase isoforms have been reported [47], in which amino terminus has an NLS in one of the isoforms (**Figure 6**). Another species of Drosophila, *D. virilis*, possesses single dUTPase isoform (510 amino acids) in pseudo-heterotrimeric format [48]. It has been shown that the *D.virilis* protein is shuttled between the nucleolus and cytoplasm compartments without a nuclear localization signal. In the human dUTPase, two distinct formats exist for nucleus and mitochondrion and they are 164 and 252 amino acids, respectively [49]. The WCR DUT gene potentially encodes two isoforms that differ in the amino-terminus. However, the sequence corresponding to known nuclear localization signal (NLS) [50] was not detected.

4.2. Comparison of activity in relevant organisms.

The WCR dUTPase revealed K_M at 0.7 μM while other eukaryotic dUTPase had it ranging between 0.4 and 13.2 μM (

Table 3). The specificity constant of the WCR dUTPase was numerically higher than that of other eukaryotes, but not significant regardless. The WCR dUTPase also exhibited a strict preference for dUTP. On the contrary, dUTPase from humans and *D. melanogaster* has been shown to have a slight activity against dTTP and dCTP [51], [52]. The 3D-model of the WCR_C dUTPase revealed that Lys92 corresponds to Gly106 and Gly110 in the *D. melanogaster* and human dUTPases (**Figure 7D**). This position surrounds M3 (**Figure 6** and **Figure 7D**), which is involved in the catalysis and interaction with the deoxyribose ring [53]. Lys residue at this position can reduce the flexibility of the loop due to possible additional hydrogen bonds. Thus, it potentially has a lower chance of accepting a nucleotide other than dUTP.

4.3. Comparative pathway analysis

dTTP is synthesized through dUMP as the main precursor [54]. The pathway for *de novo* biosynthesis of cytidine base-containing ribonucleotides is likely to be conserved both in prokaryotes and eukaryotes. However, the synthesis of uracil base-containing nucleotides is different. In *E. coli*, the ribonucleotide triphosphate reductase (RTPR) catalyzes the conversion of UTP to dUTP and CTP to dCTP. dCTP is then deaminated to synthesize dUTP or dephosphorylated to form dCMP. dUTPase dephosphorylates dUTP to obtain dUMP, which is the precursor for the synthesize dTTP. Eukaryotic organisms lack RTPR. Therefore, it is more likely that the precursor of the pyrimidine-based deoxyribonucleotides is dCDP. In eukaryotes, CTP is dephosphorylated and then reduced to dCDP. From there it can be converted to dCTP and integrated in DNA synthesis or undergo a

second dephosphorylation to produce dCMP, which is used by dCMP deaminase (DCTD) to obtain dTTP for DNA synthesis. It is unlikely that WCR can synthesize dUTP or dTTP from nucleosides (dU and dT) because it lacks the nucleoside kinases required in those reactions. Although it was not annotated by the KEGG database as part of the pyrimidine metabolism for the WCR genome, ribonucleotide reductase (RNR) is also present in the WCR genome. RNR can directly convert UDP to dUDP, which indicates that the synthesis of dUMP can be obtained by more than one pathway.

4.4. Pyrimidine metabolic pathway

Thymidylate synthase (TS), which is the only route to obtain dTMP, is inhibited by 5-flurouracil (5Fu) in chemotherapeutic treatments [55] (Figure 14). Increased expression of dUTPase, a key enzyme in the pyrimidine metabolism, has been associated with the poor efficiency of 5Fu-based chemotherapy. Therefore, pharmacological inhibition of dUTPase has been suggested as an alternative approach for chemotherapy [22]. However, dUTPase is an essential enzyme for free-living organisms. Individual knockdown of dUTPase causes death to *Saccharomyces cerevisiae* [19] and *E. coli* [20]. In eukaryotes, however, individual depletion of enzymes might not cause death. For example, downregulation of UMP synthase (UMPS) in growing potato tubers causes an overexpression of genes involved in the salvage pathway [56], preventing cell death. Overexpression of dUTPase and genes involved in the salvage pathway upon inhibition of TS and downregulation of UMPS, respectively, might suggest that dUTPase knockdown in WCR would trigger compensatory effects in the

pyrimidine metabolism of WCR such as the examples mentioned for potato tubers. The comparative pathway analysis (**Figure 14**) shows more than one pathway to obtain dUMP given the repertoire of enzymes in the WCR genome: through deamination of dCMP, the salvage pathway or reduction of UDP by Ribonucleotide Reductase (RNR).

4.5. Future direction

In this study, two potential isoforms of dUTPase were identified. The quaternary structure and the enzyme kinetics of one of the potential isoforms were described. Experiments using the Cresol Red method showed that the WCR dUTPase construct has hydrolytic activity exclusively for dUTP, which also depends on the availability of Mg^{2+}. 3D-structural analysis revealed that Lys92 of dUTPase in WCR corresponds to the Gly106 in *D. melanogaster* dUTPase and Gly110 in human dUTPase. In *D. melanogaster* and human, dUTPase is able to hydrolyze dTTP and dCTP [51], [52]. Lys92 could be responsible for the high specificity of the WCR dUTPase to dUTP by forming additional hydrogen bonds. This can be tested by performing site directed mutagenesis at this position to Gly, as is the case in Drosophila and humans. Finally, dUTPase was selected for this study due to its potential as an RNAi target. Downregulation of dUTPase in WCR larvae has been demonstrated to cause mortality [57]. However, no mortality was detected when dUTPase was knockdown in WCR adults through RNA interference (Darlington and Vélez, 2020; unpublished data).

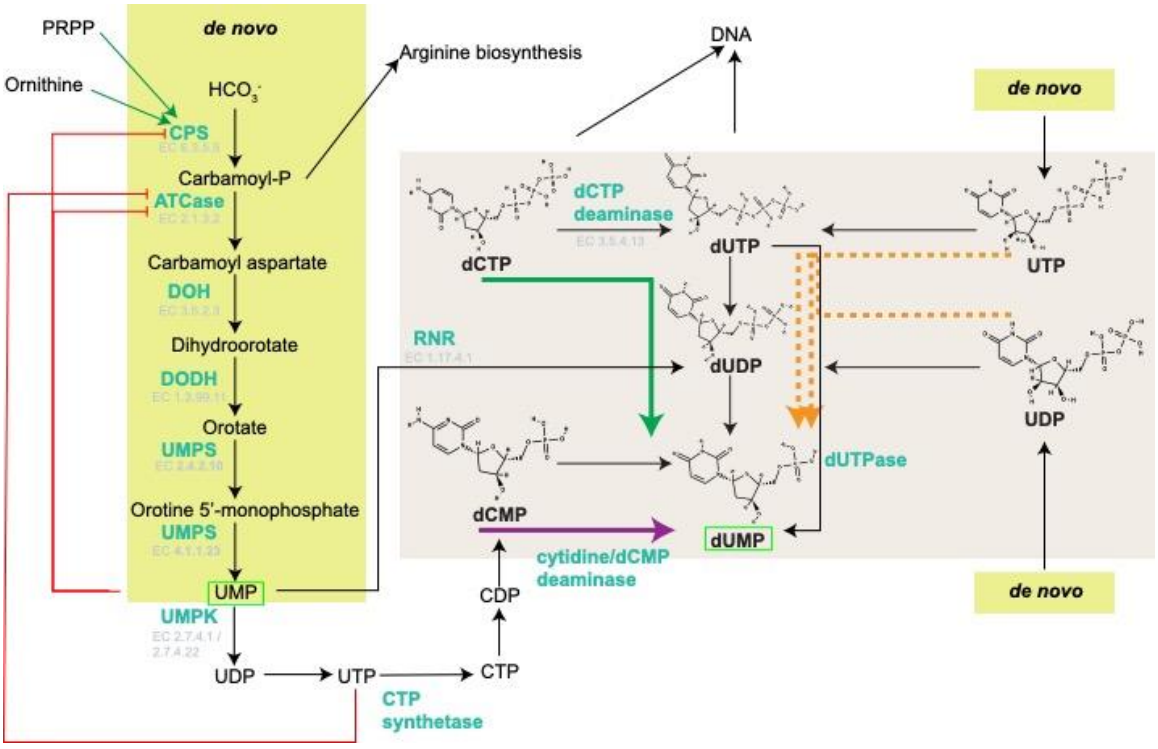

Figure 1 De novo biosynthesis of the pyrimidines (yellow panel) and pathways to obtain dUTP (brown panel). Deamination pathways based on [58].See also [59].

The three known pathways to produce dUMP (brown panel) are shown by colored arrows: deamination of dCTP (green arrow), deamination of dCMP (purple arrow), and oxidation of UTP or UDP (orange arrow). Green and orange routes must use dUTPase as the final step [59]. Cytosine deamination occurs from dCMP in eukaryotes or dCTP in some enterobacteria [58]. Formation of dUMP though reduction of UDP or UTP is a minor route in prokaryotes (dashed arrows). Blunt head red arrows indicate inhibition.

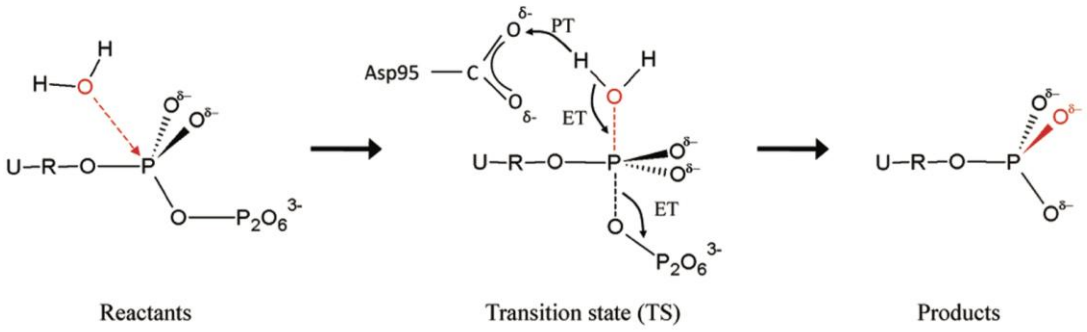

Figure 2 dUTPase catalytic mechanism.

A nucleophile attacks the α-carbon of dUTP. Source: [24]

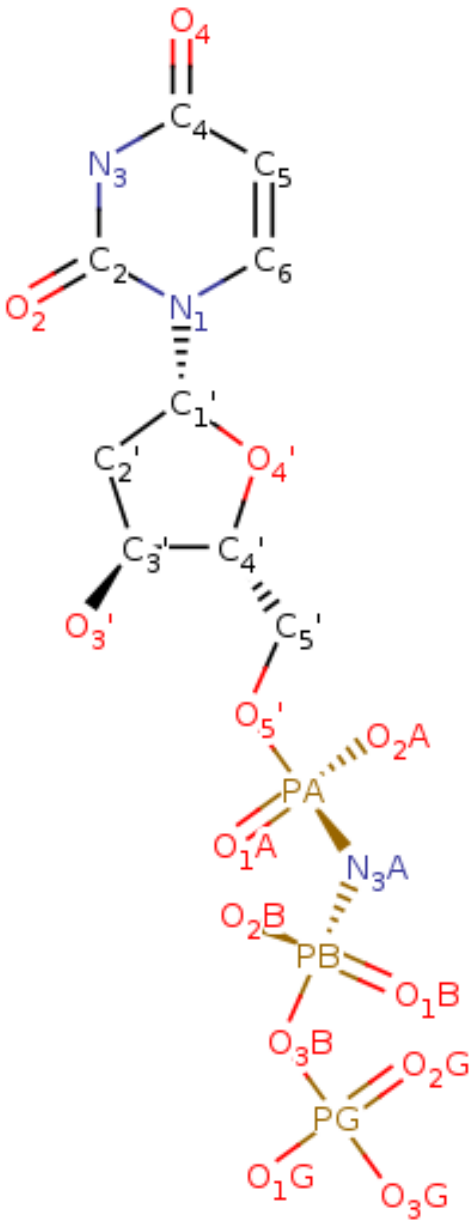

Figure 3 dUTPase inhibitor, 2′-deoxyuridine 5′-[(α,β)-imido]-triphosphate.

Figure taken from Protein Data Bank (PDB ID: 4OOP).

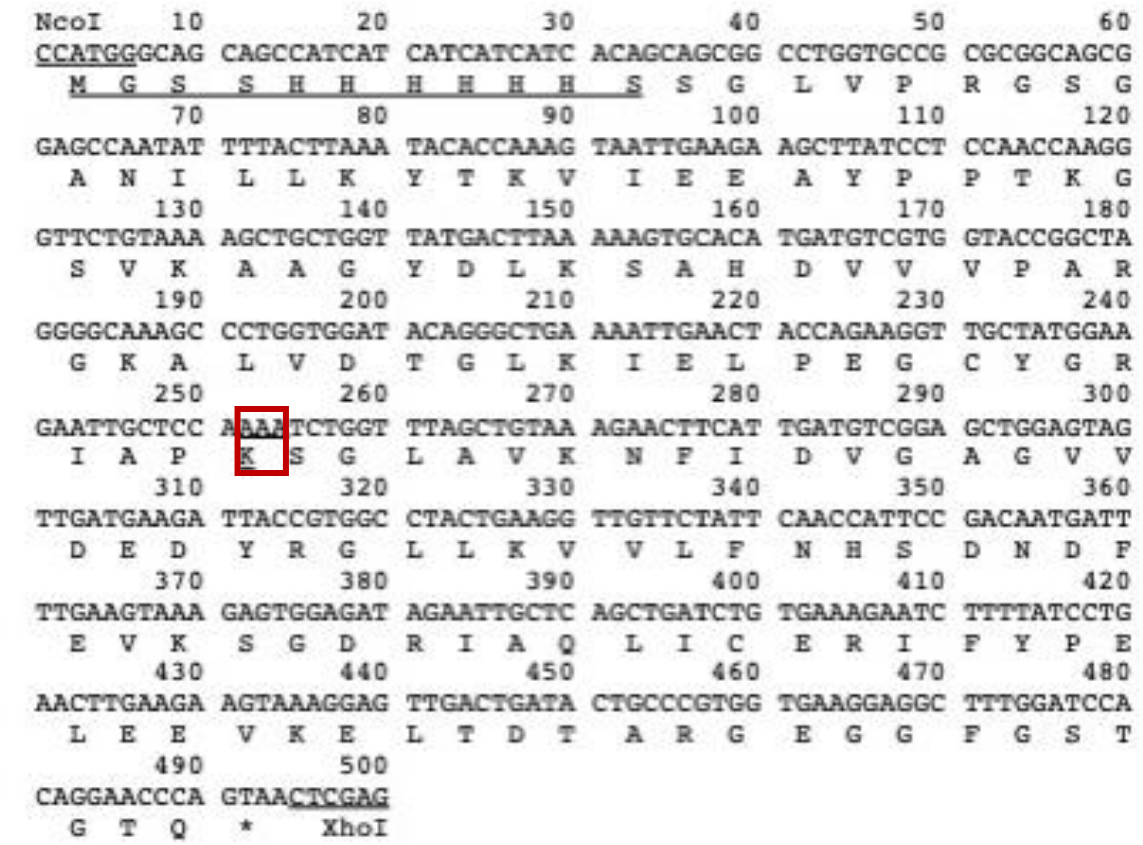

Figure 4 The nucleotide sequence of the DUT gene construct from *D. virgifera virgifera*.

The codon utilization was optimized for E. coli. The DUT gene sequence was cloned into pET-15 using NcoI and XhoI sites. Internal mutation was given to achieve Arg89Lys (boxed). After thrombin cut, N-terminus sequence including His-tag was removed.

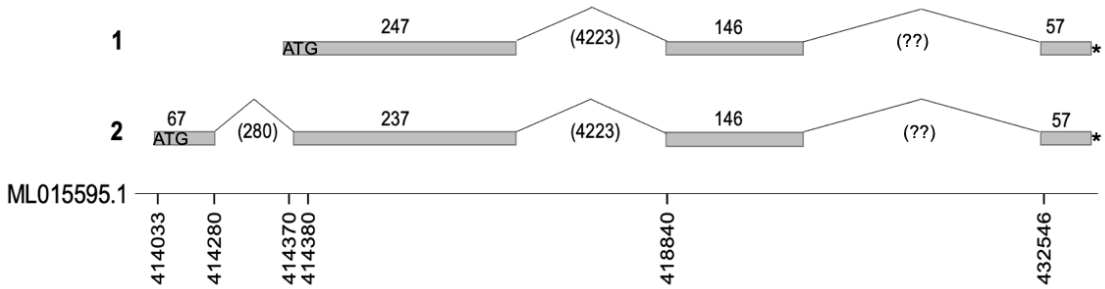

Figure 5 The DUT gene of Western corn rootworm encodes two dUTPase isoforms.
The gene structure of the two predicted isoforms of DUT transcripts in WCR were presented. The start codon is shown by ATG and the stop codon as an asterisk. The length of the last intron was not determined because the corresponding 13560 bp included many “Ns.”

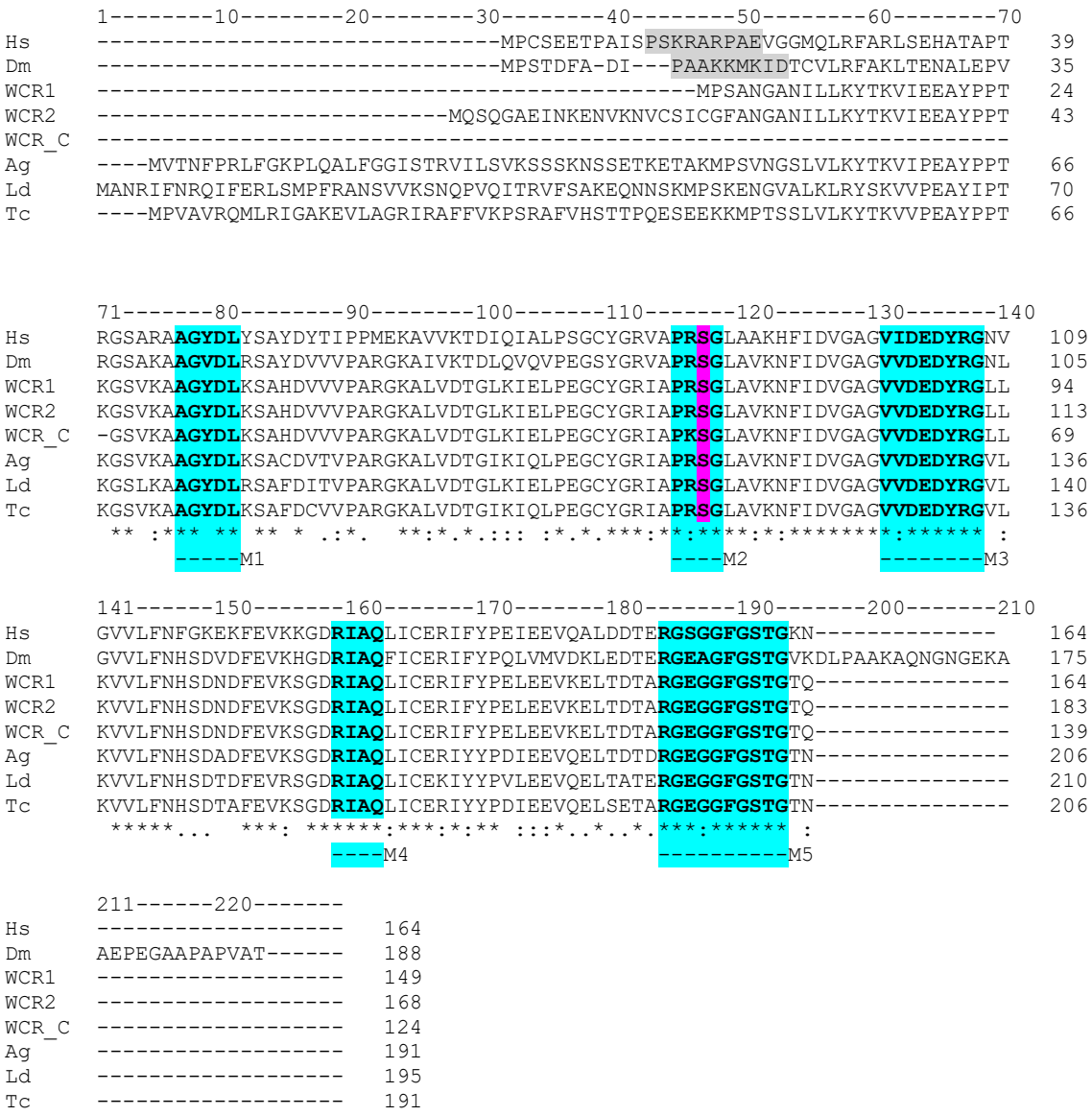

Figure 6 Structural models and sequence alignment of dUTPase.
Sequence alignment of dUTPase from human (Hs, PDBID: 3EHW), Westerm Corn Rootworm (WCR 1–2 predicted isoforms), used construct (WCR_C), *D. melanogaster* (Dm, UNIPROT_ID: Q9V3I1), *Anoplophora glabripennis* (ACC: XP_018573994.1), *Tribolium castaneum* (ACC: XP_973701.1) and *Leptinotarsa decemlineata* (ACC: XP_023012863.1). Dots (.) indicate that residues of WCR1 are identical to WCR1 and are showed as WCR_C. Cons refer similarity from T-Coffee. Five conserved motifs of trimeric dUTPases were highlighted with cyan. Resides that surround the substrate in the 3D-structure are indicated in bold. Among them, residues that have hydrogen bond with the substrate are indicated in italics. Sequences in α-helix in M2 involved in the initial grasp of substrate–water complex were highlighted in magenta [25]. Reported nuclear localization signals of dUTPase in Hs and Dm [60] were highlighted in gray.

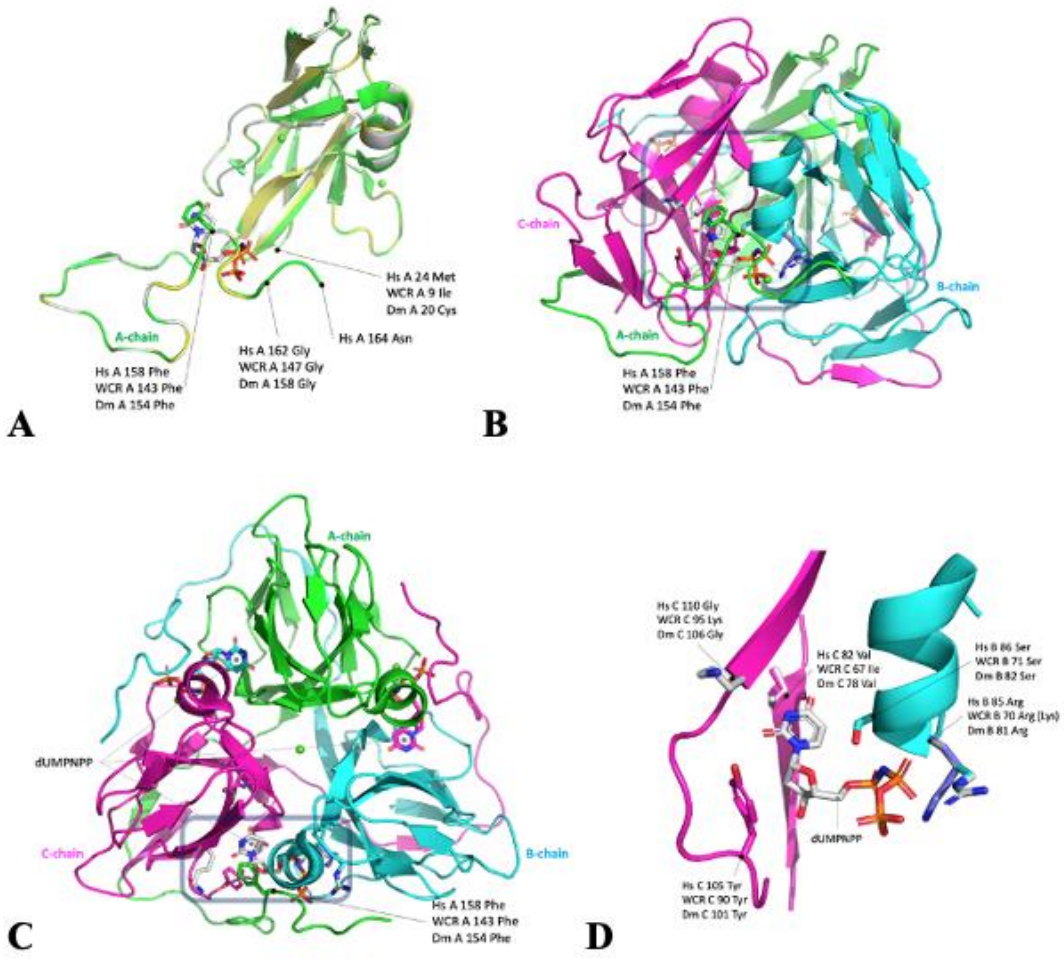

Figure 7 Structural models and sequence alignment of dUTPase.

A. Monomer structure of dUTPase. **A.** Chain structures of dUTPase from human (Hs, green), Western corn rootworm (WCR, white), and fruit fly (Dm, yellow) were superimposed. An inhibitor, dUMPNPP, and a residue 158 Phe, a lid of the active site, were shown in stick model. Small globes denote magnesium ion in the template structure. **B.** Trimer structure of dUTPase. B and C chains were added to the monomer view in A and slightly rotated about the vertical axis. Key residues in the active site were presented in stick models, and the boxed area was enlarged in D. Three active sites were indicated by the location of dUMPNPP. Enlarged area in D was boxed. **C.** Triangular view of dUTPase trimer. The molecule in B was rotated about the horizontal axis. **D.** A conventional view of the active site. The lid of the active site was removed from the scene. In the active site, only WCR dUTPase has unique residues, 67 Ile and 95 Lys, at portions corresponding to hs dUTPase at 82 Val and 110 Gly. To avoid the secondary cleavage by thrombin, the present construct has artificial substitution, Arg70Lys, at position corresponding to hs dUTPase at 88 Arg.

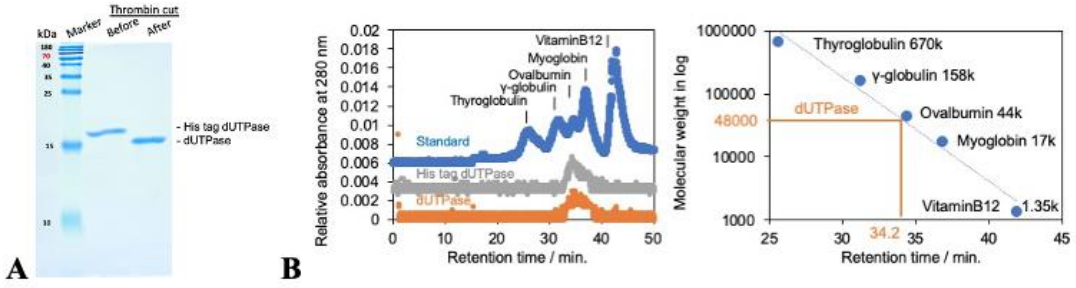

Figure 8 Results of purification and estimation of quaternary structure.

A. An 18% SDS-PAGE showing that the molecular weights for 6-histidine-tagged dUTPase and dUTPase after being cleaved by thrombin were 17.5 and 15.6 kDa, respectively. **B.** Size analysis chromatography. The inset shows the linear relationship between the retention time and the logarithm of the molecular weight of the injected samples. The orange lines indicate the retention time and the log molecular weight of the tag-free dUTPase. The estimated molecular weight of His-tag dUTPase and tag-free dUTPase were 52 and 48 kDa, respectively.

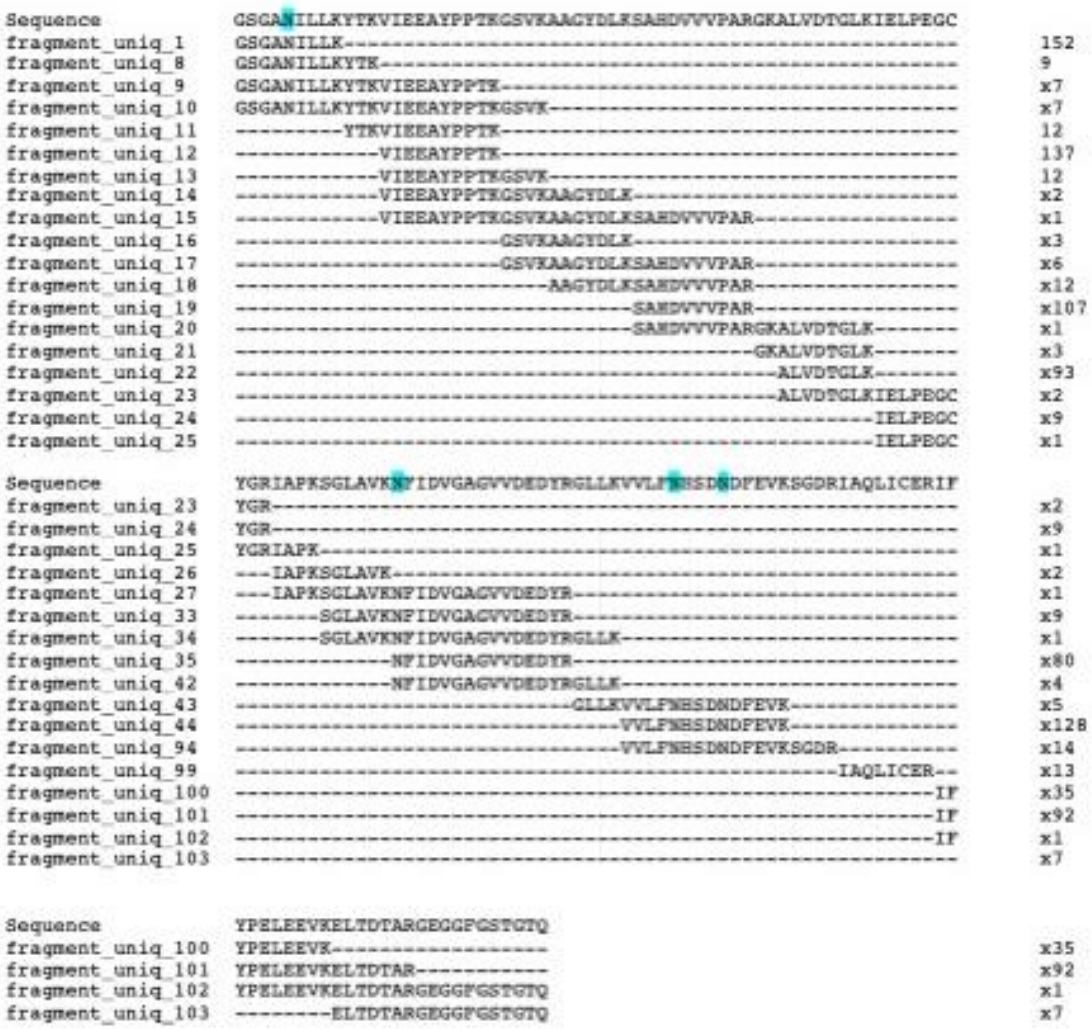

Figure 9 Identified peptides by mass spectrophotometry.

The full-length sequence was identified by MS/MS. Sixty-seven exclusive unique spectra were identified out of 968 total spectra. Likely deaminated glutamines are highlighted in cyan. All 33 unique peptide fragments are aligned against the dUTPase construct sequence. The numbers after each aligned peptide fragment represent the absolute abundance out of the 968 spectra.

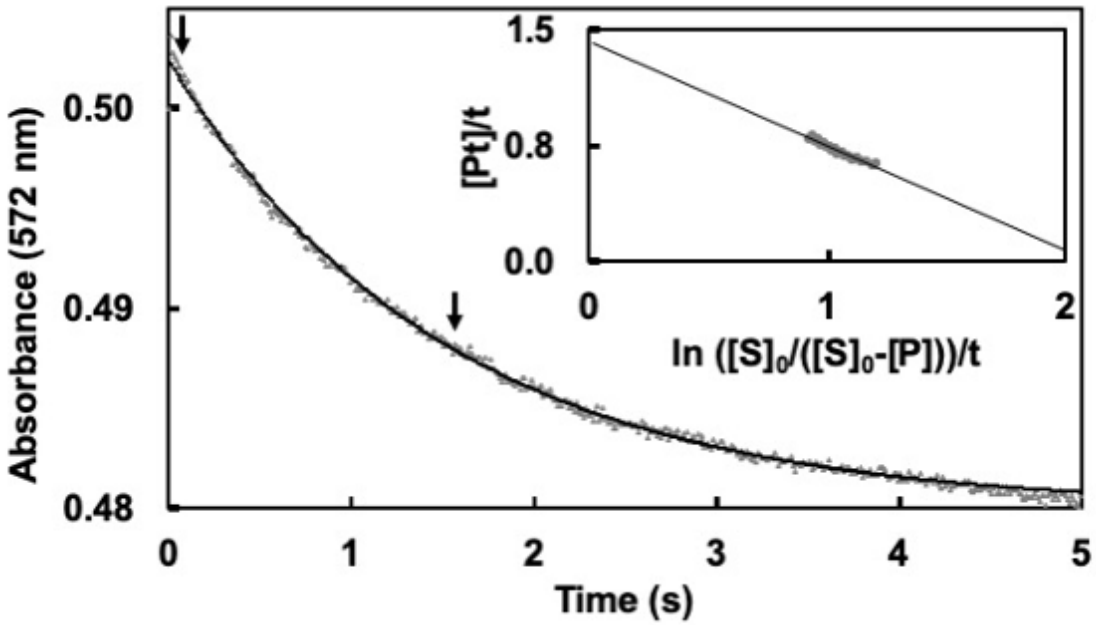

Figure 10 Complete hydrolysis of dUTP by dUTPase under multiple turnover conditions.

The reaction trace was recorded using a stopped-flow system. Observed drop of the absorbance is indicated by gray dots along the predicted regression line obtained from the seven datasets. The inset indicates the linear transformation of the data between the arrows according to the integrated Michaelis–Menten equation and the corresponding regression line (see Eq. 3).

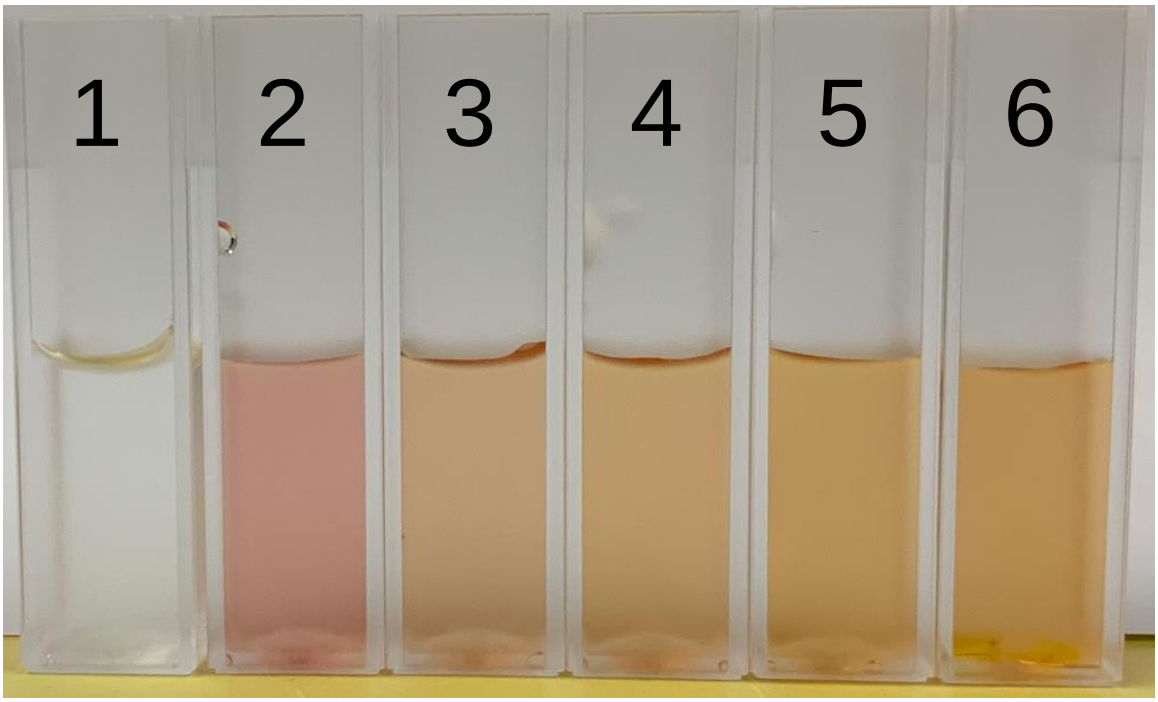

Figure 11 Cresol Red Assay.

Hydrolysis of dUTP into dUMP by WCR dUTPase produces two protons, acidifying the media. In the presence of cresol red, the media turns yellow as pH decreases. **1.** Water; **2.** Cresol Red + Substrate only, pH 8; **3-6**. Cresol Red + Substrate + WCR dUTPase (four replicates).

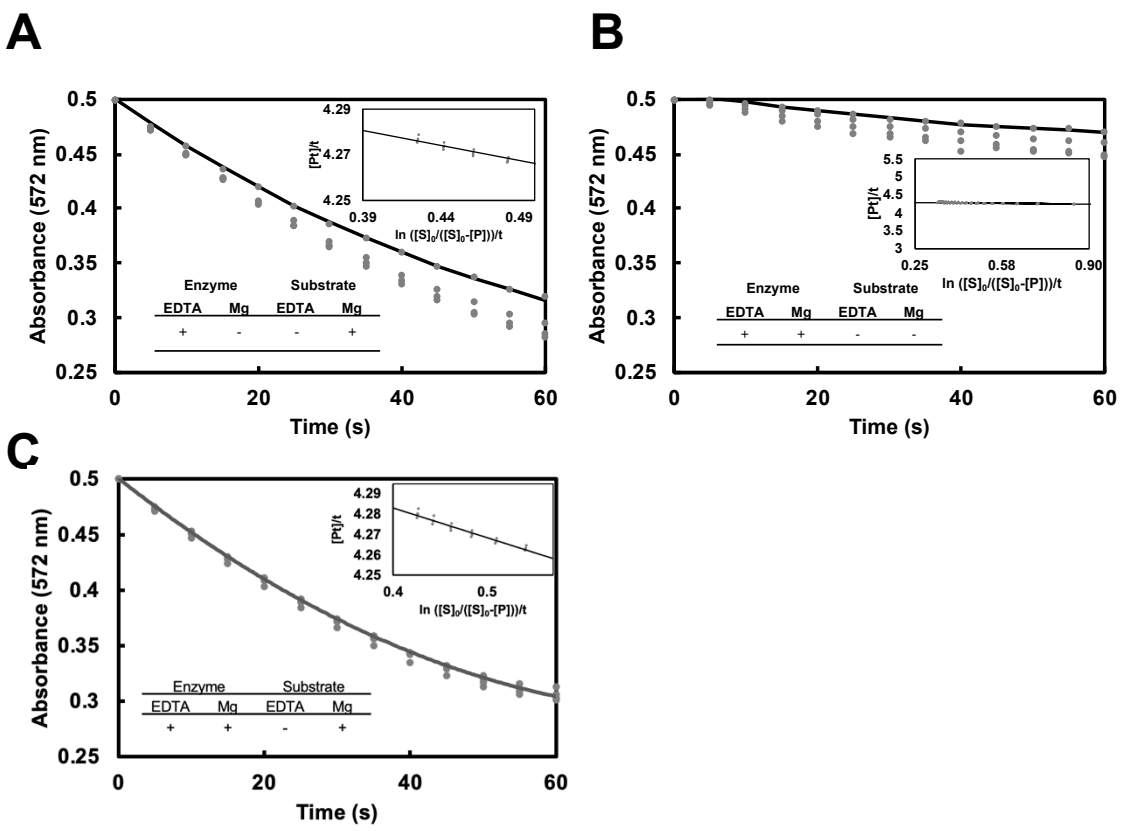

Figure 12 Hydrolysis of dUTPase under multiple turnover conditions.

A, B and C. Hydrolysis of dUTPase under multiple turnover conditions using a spectrophotometer. The recording time was 60 s with steps having a duration of 5 seconds on four independent experiments. Reaction trace was recorded at 572 nm (optical path length, 1 cm) using a conventional UV/Vis spectrophotometer Beckman Coulter DU-530 (Palo Alto, California, USA). The predicted regression line obtained from the five datasets is shown by a black line. The inset shows the linear transformation of the data according to the integrated Michaelis–Menten equation and its corresponding regression line. Each experiment consisted of reacting 20 μM of dUTP with 50 nM dUTPase in a buffer containing 5 mM of $MgCl_2$, 25 μM cresol red, and 0.25 μM bicine pH 8.2. The inset shows the linear transformation of the data between the arrows. The inset tables describe the presence or absence of EDTA and $MgCl_2$ in the experiments. The estimated values for Km and Vmax are shown in Table 2.

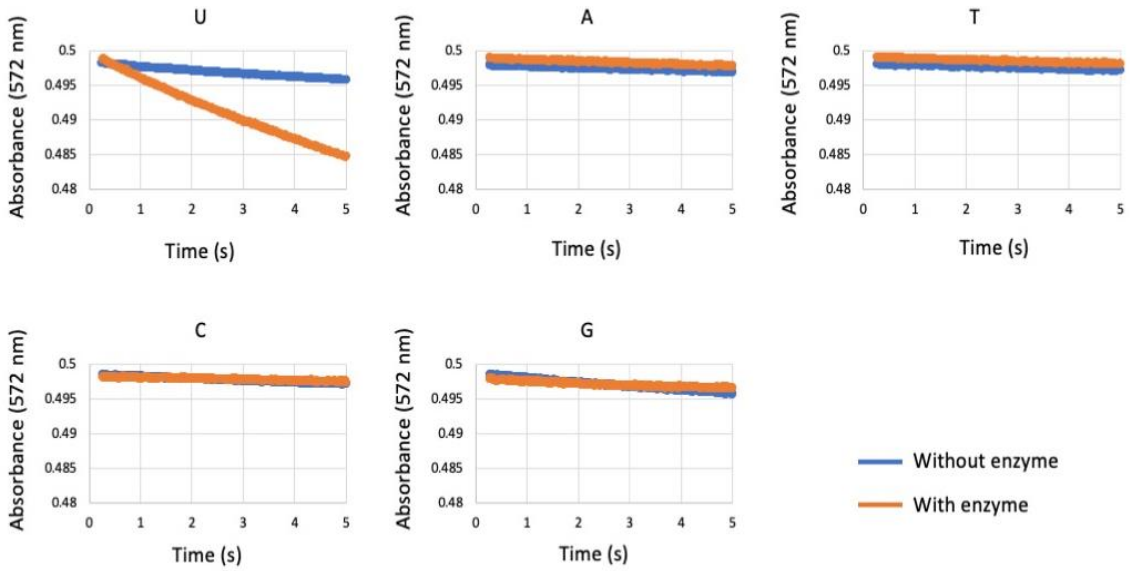

Figure 13 dUTPase specificity to dUTP.

Enzymatic and non-enzymatic reactions were carried out using a stopped-flow system. The figures show that WCR dUTPase was only able to hydrolyze dUTP (U) and not dATP (A), dTTP (T), dCTP (C) and dGTP (G).

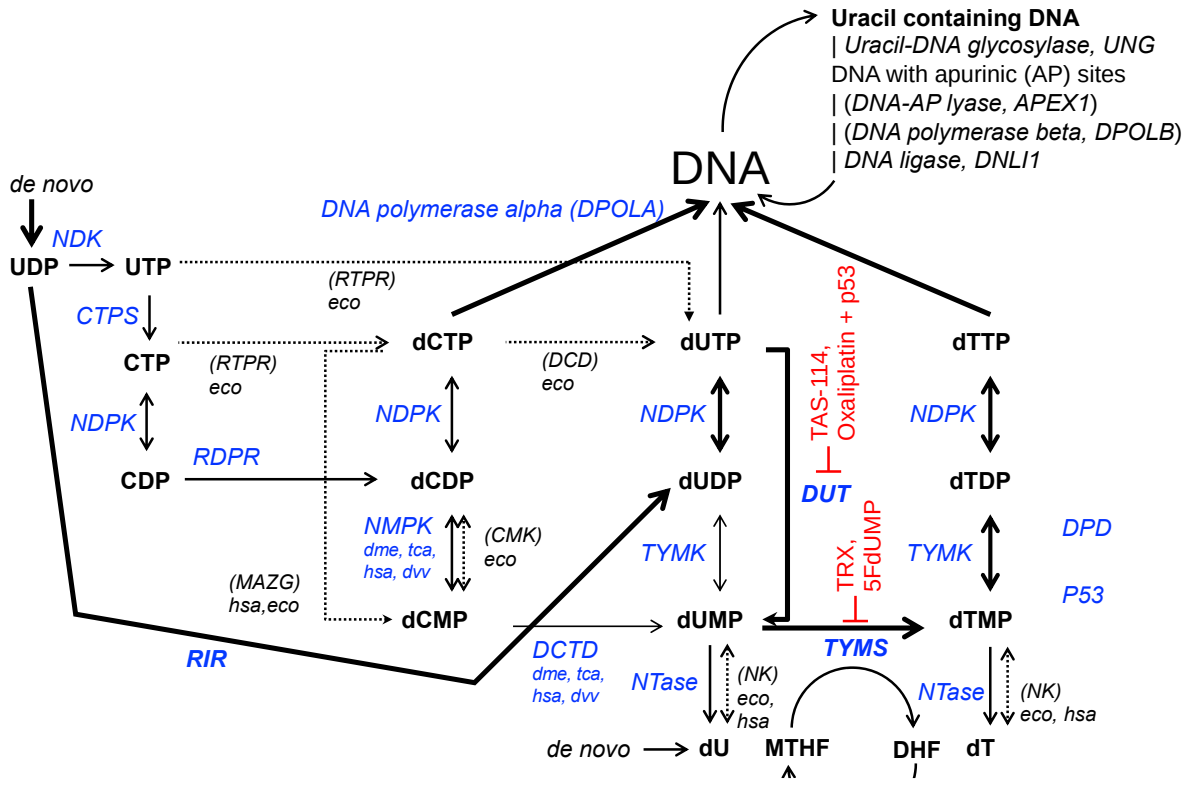

Figure 14 Proteostasis diagram for the pyrimidine biosynthesis.
DNA maintenances adapted from [61] where they compiled mainly de novo pathways in Escherichia coli (eco), Drosophila melanogaster (dme), and humans (hsa). The names of the enzymes are shown in **Table 4**. Blue is used to indicate the presence of enzymes and organisms, whereas black is used to indicate that they are not present in WCR. WCR encodes RDPR achieving dUDP production from UDP, NDPK then produces dUTP. In *E. coli*, dUTP is synthesized from CTP by the enzymes RTPR and DCD. However, WCR and other eukaryotes lack these two enzymes. These organisms also obtain dUTP from CTP by the action of five enzymes: NDK, RNR, CMPK, DCTD and DTYMK. WCR lacks the machinery to obtain dUTP from deoxyuridine. *E. coli* does not have DCTD. Uracil-DNA glycosylase is present in WCR, although it has been reported that fruit fly and other pupating insects lacked this enzyme [62]. Dotted arrows indicate pathways only present in *E. coli* or humans. 5-fluorodeoxyuridylate (5FdUMP) [63] and raltitrexed (RTX) inhibit thymidylate synthase (TYMS). Methotrexate (MTX) inhibits dihydrofolate reductase (DHFR). TAS-114 inhibits dUTPase (DUT) [64]. Moreover, oxaliplatin and p53 synergistically inhibit dUTPase [65]. The part of DNA metabolism was adapted from Hizi, A., and Herzig, E. [66].

Abbreviations on Figure 14	Full name
5FdUMP	5-fluorodeoxyuridylate (the metabolite of 5FU and 5FdUR)
DCD	dCTP deaminase
DCTD	dCMP deaminase
DUT	dUTPase
DHF	Dihydrofolate

DHFR	dihydrofolate reductase
MTHF	5,10-methylene tetrahydrofolate
MTX	Methotrexate
NDPK	nucleoside-diphosphate kinase
NK	nucleoside kinase
MAZG	nucleoside triphosphate pyrophosphohydrolase
NMPK	nucleoside monophosphate kinase
RTX	Raltitrexed
SHMT	serine hydroxymethyltransferase;
THF	Tetrahydrofolate
TYMK	dTMP kinase
TYMS	thymidylate synthase
DPD	Dihydropyrimidine dehydrogenase
P53	Cytochrome P53
RDPR	Ribonucleoside diphosphate reductase
RTPR(f)	Ribonucleotide triphosphate reductase (formate)
RNRcII	Ribonucleotide reductase class II
CMK	CMP / dCMP kinase
NTase	5’ -nucleotidase

Table 1 Insect dUTPase used to find WCR dUTPase

Order	Scientific name	Common name	NCBI Accession
Coleoptera	*Anoplophora glabripennis*	Asian long-horned beetle	XP_018573994.1
Coleoptera	*Tribolium castaneum*	Red flour beetle	XP_973701.1
Coleoptera	*Leptinotarsa decemlineata*	Colorado potato beetle	XP_023012863.1
Diptera	*Drosophila melanogaster Iso B*	Fruit fly	NP_723647.1
Diptera	*Drosophila melanogaster* Iso A	Fruit fly	NP_609479.1

Table 2 Kinetic parameters of WCR dUTPase.

Equipment	dUTPase (µM)	N	EDTA treatment	dUTP (µM)	k_M (µM)	V_{max} (µM/s)	k_{cat} (1/s)	k_{cat}/k_M (1/M*s)
Stopped-flow	5.0 x 10^{-2}	4	No	1.0	0.68 ± 0.02	1.44 ± 0.03	2.87 X 10 ± 0.54	$4.19 \times 10^7 \pm 1.22 \times 10^6$
	5.0 x 10^{-2}	5	No	5.0	0.72 ± 0.08	1.44 ± 0.07	2.88 X 10 ± 1.42	$4.00 \times 10^7 \pm 4.79 \times 10^6$
	5.0 x 10^{-2}	5	No	20	0.70 ± 0.05	1.42 ± 0.02	2.83 X 10 ± 0.40	$4.07 \times 10^7 \pm 2.90 \times 10^6$
Average					*0.70 ± 0.03*	*1.43 ± 0.03*	*2.86 X 10 ± 0.6*	*$4.09 \times 10^7 \pm 1.91 \times 10^6$*
DU-530	1.1	5	No	20	0.81 ± 0.18	1.34 ± 0.07	1.23 ± 0.06	$1.51 \times 10^6 \pm 3.40 \times 10^5$
	1.1	4	Yes	20	0.80 ± 0.37	0.98 ± 0.09	0.89 ± 0.08	$1.11 \times 10^6 \pm 5.19 \times 10^5$

Table 3 Comparison of kinetic parameters of dUTPase from different organisms.

Species	K_M (μM)	V_{max}	K_{cat} (s^{-1})	K_{cat}/K_M (M^{-1} s^{-1})	Source
S. cerevisiae	13.2 ± 0.6	31.7 Units/mg	9.6 ± 0.2	7.4×10^5	[53]
H. sapiens	3.6 ± 1.9	NR	6.7 ± 0.2	1.9×10^6	[67]
E. coli	0.5	NR	11	1.4×10^7	[68]
D. melanogaster	0.4 (0.45)[a]	NR	12 (11)[a]	3×10^7 (2.4×10^7)[a]	[51]
D. virgifera virgifera	0.70 ± 0.03	1.43 ± 0.03 μM/s	2.86 × 10 ± 0.6	$4.09 \times 10^7 \pm 1.91 \times 10^6$	This work

NR, Not reported by the author.

[a] Numbers between parentheses were calculated for the full-length construct of the *D. melanogaster dUTPase.*

Table 4 Enzymes in the pyrimidine metabolism of WCR and other orthologs shown in Figure 14.

The table describes each reaction for the *de novo* synthesis of dUTP found in *S. cerevisiae* (Sce), *H. sapiens* (hsa), *E. coli* (eco), and *D. melanogaster* (dme), and *D. virgifera virgifera* (dvv). The table was based on [61], Figure 14 of this study, and searches on KEGG and Uniprot databases. The KO and E.C. numbers were taken directly from KEGG. Unless otherwise stated, the Uniprot accession numbers were obtained by Blast searches on Uniprot using homologs of *T. castaneum* or *E. coli* found in KEGG. The enzyme names are from KEGG or based on the E.C. numbers.

Reaction		Enzyme				Organism					Substrate/Product
No	RN	Name	Gene	Db	ID	dme	tca	eco	has	dvv	
1	R00575	carbamoyl-phosphate synthase / aspartate carbamoyltransferase / dihydroorotase	[CAD] GLN-CPS	KO E.C. Uniprot	K11540 6.3.5.5 D6X207 (tca)	x	**x**	x	**x**	**x**	L-Glutamine <--> Carbamoyl-P
2	R01397	L-aspartate carbamoyltransferase	[CAD] ACT	KO E.C. Uniprot	K11540 2.1.3.2 D6X207 (tca)	x	**x**	x	**x**	**x**	Carbamoyl-P <--> N-Carbamoyl-L-aspartate
3	R01993	(S)-dihydroorotate amidohydrolase	[CAD] DOH	KO E.C. Uniprot	K11540 3.5.2.3 D6X207 (tca)	x	**x**	x	**x**	**x**	N-carbamoyl-L-aspartate <--> (S)-dihydroorotate
4	R01868	(S)-dihydroorotate:quinone oxidoreductase	DHODH	KO E.C. Uniprot	K00254 1.3.5.2 D6X3Z9 (tca)	x	**x**	x	**x**	**x**	(S)-dihydroorotate <--> orotate
5	R01870	orotidine-5'-phosphate:diphosphate phospho-alpha-D-ribosyl-transferase	UMPS	KO E.C. Uniprot	K00762 2.4.2.10 D1ZZL8 (tca)	x	**x**	x	**x**	**x**	Orotate <--> Orotidine 5'-phosphate
6	R00965	orotidine-5'-phosphate carboxy-lyase (UMP-forming)	UMPS	KO E.C. Uniprot	K13421 4.1.1.23 D1ZZL8 (tca)	x	**x**	x	**x**	**x**	orotidine 5'-phosphate <--> UMP
7	R00158	ATP:CMP(UMP) phosphotransferase	NMPK	KO E.C. Uniprot	K13800 2.7.4.14 D6W794 (tca)	x	**x**		**x**	**x**	dCDP <--> dCMP UMP <--> UDP
7a	R00158	UMP kinase	UMPK (pyrH)	KO E.C. Uniprot	K09903 2.7.4.22 P0A7E9 (eco-k12)			**x**			UMP <--> UDP
8	R00331	nucleoside-diphosphate kinase	NDPK (ndk)	KO	`	x	**x**	x	**x**	**x**	dCDP <--> dCTP dUDP <-->

				E.C. Uniprot	2.7.4.6 D6WHK2 (tca)						dUTP dTDP <--> dTTP CDP <--> CTP
9	R00573	CTP synthase	CTPS	KO E.C. Uniprot	K01937 6.3.4.2 D6WFV7 (tca)	x	**x**	x	**x**	**x**	UTP --> CTP
9a	R11592	Ribonucleotide-triphosphate reductase (formate)	RTPR (nrdD)	KO E.C. Uniprot	K21636 1.1.98.6 P28903 (eco-K12)			x			CTP --> dCTP UTP --> dUTP
10	R00331	Nucleoside-diphosphate kinase	NDPK (ndk)	KO E.C. Uniprot	K00940 2.7.4.6 D6WHK2 (tca)	x	**x**	x	**x**	**x**	dCDP <--> dCTP dUDP <--> dUTP dTDP <--> dTTP CDP <--> CTP
10.a	R11592	Ribonucleotide-triphosphate reductase (formate)	RTPR (nrdD)	KO E.C. Uniprot	K21636 1.1.98.6 P28903 (eco-K12)			x			CTP --> dCTP UTP --> dUTP
10.b	R11592	dCTP deaminase	DCD	KO E.C. Uniprot	K01494 3.5.4.13 P28248 (eco-K12)			x			dCTP --> dUTP
10.b2	R11592	dCTP diphosphatase	DCTPP1 (MAZG)	KO E.C. Uniprot	K16904 3.6.1.12 Q9H773 (has)			**x**	**x**		dCTP --> dCMP
10.c	R11592	dUTP pyrophosphatase	DUT	KO E.C. Uniprot	K01520 3.6.1.23 D6WT48 (tca)	x	**x**	x	**x**	**x**	dUTP --> dUMP
11				KO	K10807	x	**x**		**x**	**x**	CDP --> dCDP

	R04294	ribonucleoside-diphosphate reductase large subunit	RDPR (RRM1)	E.C. Uniprot	1.17.4.1 D2A2I1 (tca)						
11a	R04294	ribonucleoside-diphosphate reductase 1 subunit alpha	RDPRa(nrdA) RDPRb	KO E.C. Uniprot Uniprot	K00525 / K00526 1.17.4.1 P00452 / P39452 P69924 / P37146			x			CDP --> dCDP
12	R00512 R01665	UMP/CMP kinase	NMPK	KO E.C. Uniprot	K13800 2.7.4.14 D6W794 (tca)	x	**x**		**x**	**x**	dCDP <--> dCMP UMP <--> UDP
12.a	R00512 R01665	CMP/dCMP kinase	CMK	KO E.C. Uniprot	K00945 2.7.4.45 P0A6I0 (eco-k12)			x			dCDP <--> dCMP
13	R01663	dCMP deaminase	DCTD	KO E.C. Uniprot	K01493 3.5.4.12 A0A139WJS8 (tca)	x	**x**		**x**	**x**	dCMP --> dUMP
14	R02101	thymidylate synthase	TYMS	KO E.C. Uniprot	K00560 2.1.1.45 D7EIA1 / D2A1S6 (tca)	x	**x**	x	**x**	**x**	dCMP --> dTMP MTHF <--> DHF
15	R02094	dTMP kinase	TYMK	KO E.C. Uniprot	K00943 2.7.4.9 D6WW08 (tca)	x	**x**	x	**x**	**x**	dUMP <--> dUDP dTMP <--> dTDP
16	R00331	nucleoside-diphosphate kinase	NDPK (ndk)	KO E.C. Uniprot	K00940 2.7.4.6 D6WHK2 (tca)	x	**x**	x	**x**	**x**	dCDP <--> dCTP dUDP <--> dUTP dTDP <--> dTTP CDP <--> CTP

5. Literature Cited

[1] S. Wechsler and D. Smith, “Has resistance taken root in US corn fields? Demand for insect control,” *Am. J. Agric. Econ.*, vol. 100, no. 4, pp. 1136–1150, 2018.

[2] M. E. Gray, T. W. Sappington, N. J. Miller, J. Moeser, and M. O. Bohn, “Adaptation and Invasiveness of Western Corn Rootworm: Intensifying Research on a Worsening Pest,” *Annu. Rev. Entomol.*, 2009.

[3] L. J. Meinke, D. Souza, and B. D. Siegfried, “The Use of Insecticides to Manage the Western Corn Rootworm, Diabrotica virgifera virgifera, LeConte: History, Field-Evolved Resistance, and Associated Mechanisms,” *Insects*, vol. 12, no. 2, p. 112, 2021.

[4] U. S. EPA, “Biopesticides registration action document-Bacillus thuringiensis plant-incorporated protectants,” *Environ. Assess.*, pp. IIC2–IIC16, 2001.

[5] A. J. Gassmann *et al.*, “Field-evolved resistance by western corn rootworm to multiple Bacillus thuringiensis toxins in transgenic maize,” *Proc. Natl. Acad. Sci.*, 2014.

[6] A. J. Gassmann, “Resistance to Bt Maize by Western Corn Rootworm: Effects of Pest Biology, the Pest–Crop Interaction and the Agricultural Landscape on Resistance,” *Insects*, vol. 12, no. 2, p. 136, 2021.

[7] D. S. Wangila, A. J. Gassmann, J. L. Petzold-Maxwell, B. W. French, and L. J. Meinke, “Susceptibility of Nebraska western corn rootworm (Coleoptera: Chrysomelidae) populations to Bt corn events,” *J. Econ.*

Entomol., 2015.

[8] J. Hou *et al.*, “Engineering of Bacillus thuringiensis cry proteins to enhance the activity against western corn rootworm,” *Toxins (Basel).*, vol. 11, no. 3, p. 162, 2019.

[9] W. Moar *et al.*, “Cry3Bb1-Resistant western corn rootworm, diabrotica virgifera virgifera (LeConte) does not exhibit cross-resistance to DvSnf7 dsRNA,” *PLoS One*, 2017.

[10] J. Gerhart, “From feedback inhibition to allostery: The enduring example of aspartate transcarbamoylase,” *FEBS Journal*. 2014.

[11] M. E. Jones, “Pyrimidine Nucleotide Biosynthesis in Animals: Genes, Enzymes, and Regulation of UMP Biosynthesis,” *Annu. Rev. Biochem.*, 1980.

[12] H. Kim, R. E. Kelly, and D. R. Evans, “The structural organization of the hamster multifunctional protein CAD. Controlled proteolysis, domains, and linkers,” *J. Biol. Chem.*, 1992.

[13] J. A. Hermoso, “Getting CAD in shape: The atomic structure of human dihydroorotase domain,” *Structure*. 2014.

[14] A. Grande-García, N. Lallous, C. Díaz-Tejada, and S. Ramón-Maiques, “Structure, functional characterization, and evolution of the dihydroorotase domain of human CAD,” *Structure*, 2014.

[15] I. Lieberman, “Enzymatic amination of uridine triphosphate to cytidine triphosphate,” *J. Biol. Chem.*, vol. 222, no. 2, pp. 765–775, 1956.

[16] S.-H. HUANG *et al.*, “Human dTMP kinase: gene expression and

enzymatic activity coinciding with cell cycle progression and cell growth," *DNA Cell Biol.*, vol. 13, no. 5, pp. 461–471, 1994.

[17] A. N. Lane and T. W.-M. Fan, "Regulation of mammalian nucleotide metabolism and biosynthesis," *Nucleic Acids Res.*, vol. 43, no. 4, pp. 2466–2485, 2015.

[18] C. W. Kafer, "Characterization of the de novo pyrimidine biosynthetic pathway in Arabidopsis thaliana," Digital Repository@ Iowa State University, http://lib. dr. iastate. edu, 2002.

[19] M. H. Gadsden, E. M. McIntosh, J. C. Game, P. J. Wilson, and R. H. Haynes, "dUTP pyrophosphatase is an essential enzyme in Saccharomyces cerevisiae.," *EMBO J.*, vol. 12, no. 11, pp. 4425–4431, 1993.

[20] H. H. el-Hajj, H. Zhang, and B. Weiss, "Lethality of a dut (deoxyuridine triphosphatase) mutation in Escherichia coli.," *J. Bacteriol.*, vol. 170, no. 3, pp. 1069–1075, 1988.

[21] R. D. Ladner, "The role of dUTPase and uracil-DNA repair in cancer chemotherapy.," *Curr. Protein Pept. Sci.*, 2001.

[22] A. Hagenkort *et al.*, "dUTPase inhibition augments replication defects of 5-Fluorouracil," *Oncotarget*, vol. 8, no. 14, p. 23713, 2017.

[23] A. Horváth *et al.*, "DUTPase expression correlates with cell division potential in Drosophila melanogaster," *FEBS J.*, 2015.

[24] O. Barabas *et al.*, "Catalytic mechanism of α-phosphate attack in dUTPase is revealed by X-ray crystallographic snapshots of distinct intermediates,

31P-NMR spectroscopy and reaction path modelling," *Nucleic Acids Res.*, vol. 41, no. 22, pp. 10542–10555, 2013.

[25] N. Inoguchi *et al.*, "Structural insights into the mechanism defining substrate affinity in Arabidopsis thaliana dUTPase: The role of tryptophan 93 in ligand orientation," *BMC Res. Notes*, 2015.

[26] T. Persson, G. Larsson, and P. O. Nyman, "Synthesis of 2′-deoxyuridine 5′-(α, β-imido) triphosphate: a substrate analogue and potent inhibitor of dUTPase," *Bioorg. Med. Chem.*, vol. 4, no. 4, pp. 553–556, 1996.

[27] S. Eyun *et al.*, "Molecular evolution of glycoside hydrolase genes in the western corn rootworm (Diabrotica virgifera virgifera)," *PLoS One*, 2014.

[28] C. Camacho *et al.*, "BLAST+: architecture and applications," *BMC Bioinformatics*, vol. 10, no. 1, pp. 1–9, 2009.

[29] C. Notredame, D. G. Higgins, and J. Heringa, "T-Coffee: A novel method for fast and accurate multiple sequence alignment," *J. Mol. Biol.*, vol. 302, no. 1, pp. 205–217, 2000.

[30] A. Waterhouse *et al.*, "SWISS-MODEL: homology modelling of protein structures and complexes," *Nucleic Acids Res.*, vol. 46, no. W1, pp. W296–W303, 2018.

[31] P. Benkert, M. Biasini, and T. Schwede, "Toward the estimation of the absolute quality of individual protein structure models," *Bioinformatics*, vol. 27, no. 3, pp. 343–350, 2011.

[32] A. Bordogna, A. Pandini, and L. Bonati, "Predicting the accuracy of protein–ligand docking on homology models," *J. Comput. Chem.*, vol. 32,

no. 1, pp. 81–98, 2011.

[33] L. R. Forrest, C. L. Tang, and B. Honig, “On the accuracy of homology modeling and sequence alignment methods applied to membrane proteins,” *Biophys. J.*, vol. 91, no. 2, pp. 508–517, 2006.

[34] L. Badalucco, I. Poudel, M. Yamanishi, C. Natarajan, and H. Moriyama, “Crystallization of Chlorella deoxyuridine triphosphatase,” *Acta Crystallogr. Sect. F Struct. Biol. Cryst. Commun.*, 2011.

[35] M. Bajaj and H. Moriyama, “Purification, crystallization and preliminary crystallographic analysis of deoxyuridine triphosphate nucleotidohydrolase from Arabidopsis thaliana,” *Acta Crystallogr. Sect. F Struct. Biol. Cryst. Commun.*, 2007.

[36] K. Homma and H. Moriyama, “Crystallization and crystal-packing studies of Chlorella virus deoxyuridine triphosphatase,” *Acta Crystallogr. Sect. F Struct. Biol. Cryst. Commun.*, 2009.

[37] A. Keller, A. I. Nesvizhskii, E. Kolker, and R. Aebersold, “Empirical statistical model to estimate the accuracy of peptide identifications made by MS/MS and database search,” *Anal. Chem.*, 2002.

[38] A. I. Nesvizhskii, A. Keller, E. Kolker, and R. Aebersold, “A statistical model for identifying proteins by tandem mass spectrometry,” *Anal. Chem.*, 2003.

[39] G. Larsson, P. O. Nyman, and J. O. Kvassman, “Kinetic characterization of dUTPase from Escherichia coli,” *J. Biol. Chem.*, 1996.

[40] R. J. Foster and C. Niemann, “The evaluation of the kinetic constants of enzyme catalyzed reactions,” *Proc. Natl. Acad. Sci. U. S. A.*, vol. 39, no.

10, p. 999, 1953.

[41] M. Kanehisa, Y. Sato, and K. Morishima, “BlastKOALA and GhostKOALA: KEGG Tools for Functional Characterization of Genome and Metagenome Sequences,” *J. Mol. Biol.*, 2016.

[42] J. Thurmond *et al.*, “FlyBase 2.0: The next generation,” *Nucleic Acids Res.*, 2019.

[43] L. Wang, S. Wang, Y. Li, M. S. R. Paradesi, and S. J. Brown, “BeetleBase: The model organism database for Tribolium castaneum,” *Nucleic Acids Res.*, 2007.

[44] Z. D. Blount, “The unexhausted potential of E. coli,” *eLife*. 2015.

[45] M. Kanehisa and Y. Sato, “KEGG Mapper for inferring cellular functions from protein sequences,” *Protein Sci.*, 2019.

[46] B. G. Vértessy and J. Tóth, “Keeping uracil out of DNA: physiological role, structure and catalytic mechanism of dUTPases,” *Acc. Chem. Res.*, vol. 42, no. 1, pp. 97–106, 2009.

[47] V. Muha, I. Zagyva, Z. Venkei, J. Szabad, and B. G. Vértessy, “Nuclear localization signal-dependent and-independent movements of Drosophila melanogaster dUTPase isoforms during nuclear cleavage,” *Biochem. Biophys. Res. Commun.*, vol. 381, no. 2, pp. 271–275, 2009.

[48] G. Róna *et al.*, “NLS copy-number variation governs efficiency of nuclear import - Case study on dUTPases,” *FEBS J.*, 2014.

[49] R. D. Ladner and S. J. Caradonna, “The human dUTPase gene encodes both nuclear and mitochondrial isoforms: differential expression of the

isoforms and characterization of a cDNA encoding the mitochondrial species," *J. Biol. Chem.*, vol. 272, no. 30, pp. 19072–19080, 1997.

[50] V. Muha *et al.*, "Uracil-containing DNA in Drosophila: stability, stage-specific accumulation, and developmental involvement," *PLoS Genet*, vol. 8, no. 6, p. e1002738, 2012.

[51] J. Kovári *et al.*, "Altered active site flexibility and a structural metal-binding site in eukaryotic dUTPase: Kinetic characterization, folding, and crystallographic studies of the homotrimeric Drosophila enzyme," *J. Biol. Chem.*, 2004.

[52] I. Quesada-Soriano *et al.*, "Kinetic properties and specificity of trimeric Plasmodium falciparum and human dUTPases," *Biochimie*, 2010.

[53] A. Tchigvintsev *et al.*, "Structure and activity of the Saccharomyces cerevisiae dUTP pyrophosphatase DUT1, an essential housekeeping enzyme," *Biochem. J.*, vol. 437, no. 2, pp. 243–253, 2011.

[54] R. Hirmondo, A. Lopata, E. V. Suranyi, B. G. Vertessy, and J. Toth, "Differential control of dNTP biosynthesis and genome integrity maintenance by the dUTPase superfamily enzymes," *Sci. Rep.*, 2017.

[55] R. B. Diasio and M. R. Johnson, "The role of pharmacogenetics and pharmacogenomics in cancer chemotherapy with 5-fluorouracil," *Pharmacology*, vol. 61, no. 3, pp. 199–203, 2000.

[56] P. Geigenberger *et al.*, "Inhibition of de novo pyrimidine synthesis in growing potato tubers leads to a compensatory stimulation of the pyrimidine salvage pathway and a subsequent increase in biosynthetic

performance," *Plant Cell*, vol. 17, no. 7, pp. 2077–2088, 2005.

[57] E. Knorr *et al.*, "Gene silencing in Tribolium castaneum as a tool for the targeted identification of candidate RNAi targets in crop pests," *Sci. Rep.*, 2018.

[58] C. F. Beck, A. R. Eisenhardt, and J. Neuhard, "Deoxycytidine triphosphate deaminase of Salmonella typhimurium. Purification and characterization.," *J. Biol. Chem.*, vol. 250, no. 2, pp. 609–616, 1975.

[59] D. Prangishvili *et al.*, "Biochemical and phylogenetic characterization of the dUTPase from the archaeal virus SIRV," *J. Biol. Chem.*, vol. 273, no. 11, pp. 6024–6029, 1998.

[60] Z. Bozóky *et al.*, "Calpain-catalyzed proteolysis of human dUTPase specifically removes the nuclear localization signal peptide," *PLoS One*, vol. 6, no. 5, p. e19546, 2011.

[61] G. Róna *et al.*, "Detection of uracil within DNA using a sensitive labeling method for in vitro and cellular applications," *Nucleic Acids Res.*, 2016.

[62] W. A. Deutsch, "Why do pupating insects lack an activity for the repair of uracil-containing DNA? One explanation involves apoptosis," *Insect Mol. Biol.*, vol. 4, no. 1, pp. 1–5, 1995.

[63] R. D. Ladner *et al.*, "dUTP nucleotidohydrolase isoform expression in normal and neoplastic tissues: association with survival and response to 5-fluorouracil in colorectal cancer," *Cancer Res.*, vol. 60, no. 13, pp. 3493–3503, 2000.

[64] T. Utsugi, "New challenges and inspired answers for anticancer drug

discovery and development," *Jpn. J. Clin. Oncol.*, vol. 43, no. 10, pp. 945–953, 2013.

[65] P. M. Wilson, W. Fazzone, M. J. LaBonte, H.-J. Lenz, and R. D. Ladner, "Regulation of human dUTPase gene expression and p53-mediated transcriptional repression in response to oxaliplatin-induced DNA damage," *Nucleic Acids Res.*, vol. 37, no. 1, pp. 78–95, 2009.

[66] A. Hizi and E. Herzig, "dUTPase: the frequently overlooked enzyme encoded by many retroviruses," *Retrovirology*, vol. 12, no. 1, pp. 1–15, 2015.

[67] J. Tóth, B. Varga, M. Kovács, A. Málnási-Csizmadia, and B. G. Vértessy, "Kinetic mechanism of human dUTPase, an essential nucleotide pyrophosphatase enzyme," *J. Biol. Chem.*, 2007.

[68] O. Barabás, V. Pongrácz, J. Kovári, M. Wilmanns, and B. G. Vértessy, "Structural insights into the catalytic mechanism of phosphate ester hydrolysis by dUTPase," *J. Biol. Chem.*, vol. 279, no. 41, pp. 42907–42915, 2004.